

Mobility of Copper in Binding Sites in Rabbit Liver Metallothionein 2

Anna Rae Green and Martin J. Stillman*

Department of Chemistry, The University of Western Ontario, London, Ontario, Canada N6A 5B7

Received May 4, 1995[⊗]

We describe the first direct evidence for mobility of Cu(I) atoms within the metal binding sites in mammalian metallothionein based on temporal changes in the emission spectrum of Cu_n-MT ($n = 1-20$) in the 600 nm region. The emission intensities are specifically dependent on the temperature and on the metal:protein molar ratio between 1 Cu(I), 12 Cu(I), and 20 Cu(I) [Green, A. R.; Presta, A. P.; Gasyana, Z.; Stillman, M. J. *Inorg. Chem.* **1994**, *33*, 4159–4168]. We report that this emission spectral intensity systematically changes with time in the period following the initial binding of Cu(I) to rabbit liver Zn₇-MT that can be interpreted on a molecular level in terms of the adoption by Cu(I) of different copper–thiolate cluster structures within the binding site over a period of 18 min (at room temperature) following initial binding of the Cu(I) atoms. The kinetic traces show three significantly different trends depending on the Cu(I):MT ratio. Quantitative analysis shows that the rate of this reaction slows considerably when Cu–S_{cys}–Cu bridges must form. After an initial rise in the emission intensity during the first 5 min, the emission intensity either (i) decreases (1–8 Cu(I)), (ii) increases (9–12 Cu(I)), or (iii) remains constant (13–20 Cu(I)). The latter two trends in particular confirm the stability of the copper(I)-containing protein over time. Both qualitative and quantitative interpretation show that the final structure adopted is not the same as that formed immediately after the Cu(I) binds to the thiolate groups in Zn-MT for all metal loading ratios between 1 and 12 Cu(I). The data confirm that Cu(I) initially binds to Zn₇-MT in both the α and β domains in a noncooperative, random manner. After equilibration, the Cu(I) atoms rearrange to fill the less emissive β domain preferentially. This rearrangement is similar to that observed for Cd(II) during the formation of Cd₄-MT α -fragment when Cd(II) is added to Zn₇-MT [Stillman, M. J.; Zelazowski, A. J. *Biochem. J.* **1989**, *262*, 181–188] and accounts for the decrease in emission with time as 1–8 Cu(I) are added to Zn₇-MT. The data for 1–12 Cu(I) can be interpreted on a molecular level in terms of the mobility of bound Cu(I) between different sites in the protein and in terms of the flexibility of the peptide chain providing the first direct spectroscopic evidence that Cu(I) atoms migrate between thiolate cluster sites following initial binding. The Cu(I) bound in the α domain in the kinetically-controlled domain-distributed product migrates to the β domain to form the domain-specific thermodynamically-controlled product. The data thus provide evidence for the origin of the previously reported domain specificity for Cu(I) binding to Zn-MT. Further rearrangements by the peptide backbone account for the increase in emission intensity with time as 9–12 Cu(I) are added to Zn₇-MT.

Introduction

Metallothioneins (MT) are a class of proteins characterized by a high cysteine content and an absence of both aromatic amino acids and disulfide bonds.¹ A key feature is that the tertiary structure of the metallated protein is completely dependent on the formation of metal–thiolate bonds in the metal binding sites. A wide range of metals bind to the apo-protein (metal-free metallothionein) or displace an existing metal.² For example, cadmium binds to both mammalian apo-MT and to mammalian Zn₇-MT to form Cd₇-MT.³ NMR^{4,5} and X-ray diffraction studies^{6,7} have established that Zn(II) and Cd(II) bind to metallothionein with tetrahedral coordination (that is in MS₄ units) in two domains, named α and β , that are based on

M₄(S_{cys})₁₁ and M₃(S_{cys})₉ metal–thiolate cluster structures, respectively.¹ The cysteinyl thiolates bind both in a bridging manner (M–RS–M) and in a terminal manner (RS–M).

As the structural aspects of the metal-binding site within metallothionein have become well established, interest has begun to focus on the chemical reactivity of the protein. Studies of the dynamics of the metal binding reaction, of the equilibrium processes involved in metal substitution reactions and of the kinetics of competitive metal chelation by other ligands may provide important clues towards the biological function of metallothionein. ¹¹³Cd NMR spectroscopic studies on Cd–MT suggest that the metal–thiolate clusters are quite dynamic with the bound metals involved in continuous exchange between different sites.^{8,9} Competition for the metals in the metallothionein binding sites by added ligands is well-documented both *in vitro*^{10–13} and *in vivo*.^{14,15} The bimolecular nature of interprotein metal exchanges between Zn₇-MT and apo-carbonic an-

* To whom correspondence should be addressed. Tel: (519) 661-3821; Fax: (519) 661-3022; E-mail: Stillman@uwo.ca.

[⊗] Abstract published in *Advance ACS Abstracts*, March 15, 1996.

- (1) (a) Kagi, J. H. R., Kojima, Y., Eds. *Metallothionein II*, Exp. Sup. 52; Birkhauser Verlag: Basel, Switzerland, 1987. (b) Stillman, M. J., Shaw, C. F., III, Suzuki, K. T., Eds. *Metallothioneins*; VCH Publishers: New York, 1992. (c) Suzuki, K. T., Imura, N., Kimura, M., Eds. *Metallothioneins III*; Birkhauser Verlag: Basel, 1993.
- (2) Nielson, K. B.; Atkin, C. L.; Winge, D. R. *J. Biol. Chem.* **1985**, *260*, 5342–5350.
- (3) Stillman, M. J.; Cai, W.; Zelazowski, A. J. *J. Biol. Chem.* **1987**, *262*, 4538–4548.
- (4) Otvos, J. D.; Armitage, I. M. *Proc. Natl. Acad. Sci. U.S.A.* **1980**, *77*, 7094–7098.
- (5) Messerle, B. A.; Schaffer, A.; Vasak, M.; Kagi, J. H. R.; Wurthrich, K. *J. Mol. Biol.* **1992**, *225*, 433–443.
- (6) Robbins, A. H.; McRee, D. E.; Williamson, M.; Collett, S. A.; Xuong, N. H.; Furey, W. R.; Wang, B. C.; Stout, C. D. *J. Mol. Biol.* **1991**, *221*, 1269–1293.
- (7) Robbins, A. H.; Stout, C. D. In *Metallothioneins*; Stillman, M. J., Shaw, C. F., III, Suzuki, K. T., Eds.; VCH Publishers: New York, 1992; pp 31–54.
- (8) Nettesheim, D. G.; Engeseth, H. R.; Otvos, J. D. *Biochemistry* **1985**, *24*, 6744–6751.
- (9) Vasak, M. *Environ. Health Perspect.* **1986**, *65*, 157–165.
- (10) Petering, D. H.; Krezoski, S.; Villalobos, J.; Shaw, C. F., III; Otvos, J. D. In *Metallothionein II*, Exp. Sup. 52; Kagi, J. H. R., Kojima, Y., Eds.; Birkhauser Verlag: Basel, Switzerland, 1987; pp 573–580.

hydrase¹³ and between Cd₇-MT and Hg-MT¹⁶ imply that direct interaction between the proteins occurs at the site of metal binding. The accessibility of these metal sites allows metallothionein to undergo associative ligand substitution reactions which result in facile metal exchange reactions *in vitro*^{3,8,17–20} and as well, presumably, *in vivo*. Finally, little has been reported on the role of the peptide flexibility in accommodating the large number of metals that can bind to the 20S_{cys}. Optical experiments indicate that the environment of the protein influences the possible metal:protein stoichiometries that form in the binding site, for example, the formation of Cu₉Zn₂-MT₂.²⁰

This lability introduces the possibility of a change in the site of metal binding that can be induced by the addition of subsequent metals. Changes in CD spectral data between 5 and 50 °C indicate that considerable thermally-induced rearrangement takes place after Cd(II) or Ag(I) initially bind to Zn₇-MT.^{3,17,18} Optical studies using both circular dichroism and emission spectroscopy indicate that similar thermally-induced rearrangements occur when Cu(I) binds to Zn₇-MT.^{19,20} *In vitro* analytical studies suggested that for mammalian apo-MT, the β domain fills first to form the domain-specific Cu₆(S_{cys})₉ metal-thiolate cluster structure.²¹ Significantly, the optical spectral studies of Cu(I) binding to rabbit liver Zn₇-MT suggest that the prior presence of the Zn(II) in the tetrahedral sites changes this domain specificity.^{19–22} Analysis of the temperature dependence of these Cu(I) titrations indicated that Cu(I) binds initially to *both* domains.^{19,20} Following equilibration at high temperatures the first six Cu(I) are located in the β domain.¹⁹ Clearly, the Cu(I) must be able to migrate from one domain to the other. Li and Weser²³ have suggested a mechanism for copper binding that assumes random binding across both domains in the same way proposed for cadmium binding to Zn₇-MT.^{3,17}

This paper now provides the first direct spectroscopic evidence of this migration. Many techniques that can monitor the site of metal binding precisely are either too slow, or too insensitive to be useful in this case. However, for both Cu(I)- and Ag(I)-containing metallothioneins, the emission spectrum observed in the 500–600 nm region is extremely sensitive to the metal to protein stoichiometric ratio, with maxima at 12 for Cu-MT, and 12 and 17 for Ag-MT.^{19,22–26} This luminescence

has been attributed to metal-centered 3d⁹4s¹ triplet excited states, and we have shown that the excited state lifetimes of the luminescence do not depend on the Cu(I):MT ratio.²⁶

In this paper, we report that the time dependence of the intensity of the emission spectrum recorded from Cu_n-MT (*n* = 1–20) reveals that the Cu(I) is significantly mobile following initial binding. The data also show for the first time that Cu(I) atoms migrate within the α domain when both domains are filled at the Cu(I):MT = 12 point. Although there has been increasing interest in the ligand competition reactions of metallothionein,^{10–13} there has been no previous quantitative study on the kinetics of internal metal rearrangement within the protein or discussion of the effects of flexibility of the peptide chain in controlling the actual structure of the metal binding site.

Materials and Methods

Zn₇-MT was isolated from rabbit livers following *in vivo* induction procedures using aqueous zinc salts. The protein was purified using gel filtration and electrophoresis as previously described.^{3,27} Aqueous protein solutions were prepared by dissolving the protein in argon-saturated distilled water. Protein concentrations were estimated from measurements of the –SH group and zinc concentrations. These estimations were based on the assumption that there are 20 –SH groups and 7 Zn atoms in each protein molecule. The concentration of the –SH groups was determined by the spectrophotometric measurement of the colored thionitrobenzoate anion ($\epsilon_{420} = 13\,600\text{ M}^{-1}\text{ cm}^{-1}$) produced by reaction with DTNB (5,5'-dithiobis(2-nitrobenzoic acid)) in the presence of 6 M guanidine hydrochloride.²⁸ Zinc concentrations were determined by flame atomic absorption spectrometry (AAS).

Cu(I), in the form of [Cu(CH₃CN)₄]ClO₄²⁹ in a 30% (v/v) acetonitrile/water solution, was added to the argon-saturated aqueous solutions of Zn₇-MT. The final concentration of acetonitrile in the solutions was less than 4% (v/v). The number of Cu(I) and Zn(II) atoms bound to the protein after each experiment was determined by AAS analysis following chelation of the free metal by Chelex-100. Emission data were recorded on a Photon Technology Inc. LS-100 spectrometer purged with nitrogen or argon gas. Optical glass filters were placed over the excitation (Corning 7–54 or Schott BG-24) and emission slits (Corning CS 3–74 or Schott GG-420) for observation of emission in the 500–700 nm region with excitation at 300 nm. Rate constants were determined from the slope of pseudo-first-order plots of $\ln(\text{Int}(t) - \text{Int}(\infty))$ or $\ln(\text{Int}(\infty) - \text{Int}(t))$ vs time.

Results

The absorption spectra of copper metallothioneins are very broad, extending from 200 to 350 nm, superimposed on a rising background that extends to 210 nm. The absorption spectrum encompasses many overlapping individual peptide-based and ligand-to-metal charge transfer bands.^{20,22,23} Excitation into the charge transfer bands results in the appearance of a strong broad emission band centered near 600 nm at room temperature.¹⁹ The significant feature of this emission is that the intensity is entirely dependent on the presence of Cu(I) bound to the cysteinyl thiolates of the metallothionein. Thus the emission spectral intensity reports on copper binding directly from the metal binding site. Since interactions with the solvent provide a radiationless path for degrading the energy of an excited state, room temperature emission of solvated complexes is unusual.³⁰ Room temperature luminescence of inorganic Cu(I) complexes has been observed only when the metal center is protected from the solvent environment as in Cu(I) complexes with heteroaromatic ligands^{31–36} and in inorganic Cu(I) clusters.^{37–39} *Given*

- (11) Otvos, J. D.; Petering, D. H.; Shaw, C. F., III. *Comments Inorg. Chem.* **1989**, *9*, 1–35.
- (12) Petering, D. H.; Krezoski, S.; Chen, P.; Pattanaik, A.; Shaw, C. F., III. In *Metallothioneins*; Stillman, M. J.; Shaw, C. F., III; Suzuki, K. T., Eds.; VCH Publishers: New York, 1992; pp 164–185.
- (13) Li, T.-Y.; Kracker, A. J.; Shaw, C. F., III; Petering, D. H. *Proc. Natl. Acad. Sci. U.S.A.* **1980**, *77*, 6334–6338.
- (14) Cherian, M. G.; Singh, P. K.; Basinger, M. A.; Jones, S. G. *Toxicol. Appl. Pharmacol.* **1991**, *110*, 241–250.
- (15) Cherian, M. G. *Nature* **1980**, *287*, 871–872.
- (16) Johnson, B. A.; Armitage, I. M. *Inorg. Chem.* **1987**, *26*, 3139–3144.
- (17) Stillman, M. J.; Zelazowski, A. J. *J. Biol. Chem.* **1988**, *263*, 6128–6133.
- (18) Zelazowski, A. J.; Stillman, M. J. *Inorg. Chem.* **1992**, *31*, 3363–3370.
- (19) Green, A. R.; Presta, A.; Gasyna, Z.; Stillman, M. J. *Inorg. Chem.* **1994**, *33*, 4159–4168.
- (20) Presta, A.; Green, A. R.; Zelazowski, A.; Stillman, M. J. *Eur. J. Biochem.* **1995**, *227*, 226–240.
- (21) Nielson, K. B.; Winge, D. R. *J. Biol. Chem.* **1984**, *259*, 4941–4946.
- (22) (a) Stillman, M. J. In *Metallothioneins*; Stillman, M. J.; Shaw, C. F., III; Suzuki, K. T., Eds.; VCH Publishers: New York, 1992; pp 55–127. (b) Stillman, M. J. *Coord. Chem. Rev.* **1995**, *144*, 461–511.
- (23) Li, Y.-J.; Weser, U. *Inorg. Chem.* **1992**, *31*, 5526–5533.
- (24) Zelazowski, A. J.; Gasyna, Z.; Stillman, M. J. *J. Biol. Chem.* **1989**, *264*, 17091–17099.
- (25) Stillman, M. J.; Gasyna, Z. *Methods Enzymol.* **1991**, *205*, 540–555.
- (26) Gasyna, Z.; Zelazowski, A. J.; Green, A. R.; Ough, E. A.; Stillman, M. J. *Inorg. Chem. Acta* **1988**, *153*, 115–118.

- (27) Zelazowski, A. J.; Szymanska, J. A.; Witas, H. *Prep. Biochem.* **1980**, *10*, 495–505.
- (28) (a) Ellman, G. L. *Arch. Biochem. Biophys.* **1959**, *82*, 70–77. (b) Birchmeier, W.; Christen, P. *FEBS Lett.* **1971**, *18*, 209–213.
- (29) Hemmerich, P.; Sigwart, C. *Experientia* **1963**, *19*, 488–489.
- (30) Lytle, F. E. *Appl. Spectrosc.* **1970**, *24*, 319–326.

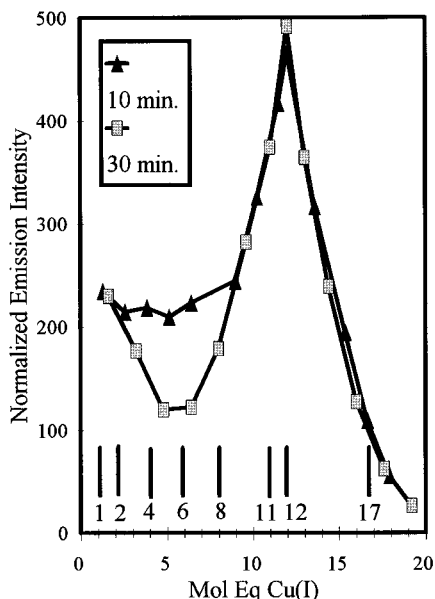


Figure 1. Normalized emission intensities as a function of the Cu(I):MT molar ratio. The dependence of the normalized emission intensity at λ_{\max} (see ref 19) calculated as [(measured intensity at λ_{\max} near 600 nm)/(Cu(I):MT molar ratio)] on the Cu(I):MT molar ratio at 19 °C in aqueous solution is shown. The *triangles* represent the intensities obtained when the solution was equilibrated for 5 min after each addition of Cu(I) before acquiring the emission spectrum. The scan took 5 min, resulting in intervals of 10 min between each addition of Cu(I). The *squares* represent the intensities obtained when the solution was equilibrated for 25 min after each addition of Cu(I) before acquiring the emission spectrum (resulting in intervals of 30 min between each addition of Cu(I)). The vertical bars in the lower part of the graph indicate the final Cu(I):MT molar ratios of the data presented in Figures 2 and 3.

this, changes in the magnitude of the emission intensity from copper-substituted metallothioneins can be attributed largely to the efficiency with which a particular metal binding structure shields the copper–thiolate cluster from the aqueous solvent. The more open or porous the structure, the more exposed the copper–thiolate cluster will be and the lower the emission intensity expected. Therefore, the effect of the $S_{\text{cys}}\text{-Cu-S}_{\text{cys}}$ cross-linking on the wrapping of the peptide chain round the metals will directly relate to the solvent access to the Cu– S_{cys} clusters.

Figure 1 shows the phenomenological basis for the conclusions reached in this paper. The results of two experiments are shown. Following excitation at 300 nm, emission spectra were measured either every 10 or every 30 minutes following sequential additions of Cu(I) to $Zn_7\text{-MT}$. The dependence of the *normalized emission intensity* (that is, intensity per mole equivalent of Cu(I) added or quantum yield expressed on a per Cu(I) basis rather than on a molecular basis) at the band centers

Table 1. Metal Content (mol equiv) of Metallothioneins

solution	$Zn_7\text{-MT} + 13\text{Cu(I)}$		$Zn_7\text{-MT}$
	Cu(I)	Zn(II)	Zn(II)
before Chelex	13.1 ± 0.1	7.0 ± 0.1	7.0 ± 0.1
after Chelex	12.9 ± 0.1	0.35 ± 0.05	7.1 ± 0.1

(between 598 and 620 nm) on the Cu(I):MT molar ratio at 20 °C is plotted in Figure 1. The emission spectrum is not significantly dependent on the excitation wavelength chosen between 270 and 330 nm. An excitation wavelength of 300 nm was chosen to ensure excitation of charge transfer, rather than peptide-based, states. The broad shape of the absorption envelope does not change as 1 to 12 Cu(I) are added to $Zn_7\text{-MT}$, rather the absorbance between 250 and 350 nm increases linearly in correspondence with the formation of Cu(I)-thiolate bonds.²⁰ The addition of 1–10 Cu(I) to $Zn_7\text{-MT}$ produces emission spectra consisting of a single broad emission band centered at 601 ± 1 nm.¹⁹ This emission band center shifts to 598 nm when 11 or 12 Cu(I) have been added and then red-shifts steeply to roughly 620 nm by the time 15 Cu(I) have been added.¹⁹ The elapsed times between Cu(I) additions in Figure 1 were chosen to best illustrate short mixing (10 min) and more complete equilibration (30 min) times. The figure shows unambiguously that the normalized emission intensities depend dramatically on the equilibration time, particularly when <9 Cu(I) have been added to the protein. Significantly, the dependence of the intensity on the molar ratio of Cu(I):MT is *not linear in either case*. We would expect the emission intensity to increase proportionately with the number of copper atoms added. This effect would produce a horizontal line in Figure 1. Clearly, this is not the case. The yield in emission intensity follows a complicated mechanism as there is an absolute *decrease in emission yield between 2 and 7 Cu(I) added* in both the 10- and 30-min data sets. A significant feature evident from the data in Figure 1 is that the temporal dependence of the emission intensity is greatest in the Cu:MT range 1–8 and least between 8 and 18.

In order to ensure that this dramatic time dependence in the emission intensity, that also depends on the Cu(I):MT ratio (as seen in Figure 1), did not arise from incomplete binding of Cu(I) over a short period of time, the metal contents of the metallothionein solutions 5 min after the addition of Cu(I) were determined as follows. A single aliquot of 13 mol equiv of Cu(I) was added to 2 mL of 10 μM $Zn_7\text{-MT}$ and the solution stirred for 5 min. A 100 mg sample of Chelex-100 resin was added to 1.5 mL of this solution and stirred for 5 min to sequester free metal ions in solution. The supernatant and the 0.5 mL of solution not exposed to Chelex were analyzed for Cu and Zn by AAS. The results of these analyses are shown in Table 1. As a control, Chelex-100 was added to 10 μM $Zn_7\text{-MT}$ alone. Chelex-100 binds free Zn(II) and Cu(I) ions up to a capacity of 22 μg of Zn(II)/mg of Chelex and 19 μg of Cu(I)/mg of Chelex.⁴⁰ The control data show that Chelex-100 does not remove Zn(II) bound to metallothionein under these conditions. The data for $Zn_7\text{-MT} + 13\text{Cu(I)}$ show that complete replacement of the Zn(II) bound to the protein by the 12 Cu(I) occurs and that there is no free Cu(I) in solution after 5 min. Figure 1 in our previous report¹⁹ provides full details of the stoichiometric replacement of Zn(II) by Cu(I). At low temperatures, a linear relationship between Cu(I) added and Zn(II) displaced is found, with all Zn(II) displaced at the 12 Cu(I) point. At warm temperatures (>15 °C) hysteresis is observed in the Zn(II)-remaining vs Cu(I)-added plot. We

- (31) Gushurst, A. K. I.; McMillin, D. R.; Dietrich-Buchecker, C. O.; Sauvage, J.-P. *Inorg. Chem.* **1989**, *28*, 4070–4072.
- (32) Palmer, C. E. A.; McMillin, D. R. *Inorg. Chem.* **1987**, *26*, 3837–3840.
- (33) Dietrich-Buchecker, C. O.; Marnot, P. A.; Sauvage, J.-P.; Kirchoff, J. R.; and McMillin, D. R. *J. Chem. Soc., Chem. Commun.* **1983**, 513–515 (Errata: **1984**, 204).
- (34) Blaskie, M. W.; McMillin, D. R. *Inorg. Chem.* **1980**, *19*, 3519–3522.
- (35) Rader, R. A.; McMillin, D. R.; Buckner, M. T.; Matthews, T. G.; Casadonte, D. J.; Lengel, R. K.; Whittaker, S. B.; Darmon, L. M.; Lytle, F. E. *J. Am. Chem. Soc.* **1981**, *103*, 5906–5912.
- (36) Everly, R. M.; Ziessel, R.; Suffert, J.; McMillin, D. R. *Inorg. Chem.* **1991**, *30*, 559–561.
- (37) Henary, M.; Zink, J. I. *J. Am. Chem. Soc.* **1989**, *111*, 7407–7411.
- (38) Vogler, A.; Kunkely, H. *J. Am. Chem. Soc.* **1986**, *108*, 7211–7212.
- (39) Sabin, F.; Ryu, C. K.; Ford, P. C.; Vogler, A. *Inorg. Chem.* **1992**, *31*, 1941–1945.

(40) Cai, W.; Stillman, M. J. *Inorg. Chim. Acta* **1988**, *152*, 111–115.

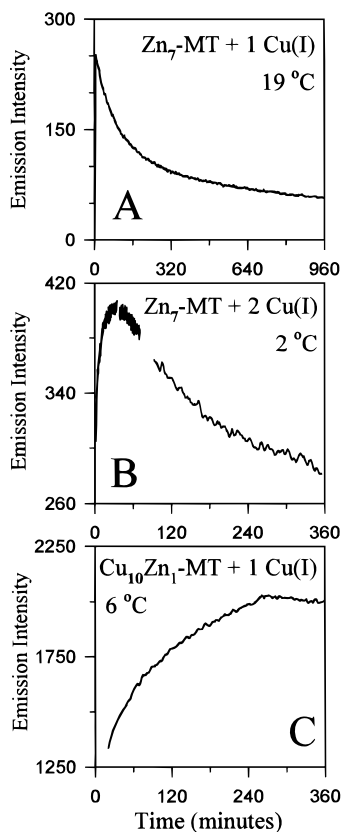


Figure 2. Emission Intensity as a function of time for several hours after the addition of Cu(I) to metallothionein solutions. (A) 1 mol equiv of Cu(I) was added through a septum to an argon-saturated solution of 30 μ M Zn₇-MT at 19 °C and the intensity at 600 nm was measured every minute for 16 h (960 min). (B) 2 mol equiv of Cu(I) was added to an argon-saturated solution of 10 μ M Zn₇-MT at 2 °C and the emission intensity at 600 nm monitored over 6 h (360 min). Since the proprietary software package controlling the LS-100 only allows for the collection of 999 data point per trace, the data were obtained in three separate traces using increments of 3, 3, and 60 s for the first, second, and third traces, respectively. The blank areas represent the periods in which the spectrometer was reinitialized and no data points could be collected. (C) The emission intensity at 600 nm was monitored over 6 h following the addition of 1 mol equiv of Cu(I) to 10 μ M Cu₁₀Zn₁-MT at 6 °C.

interpreted these effects in terms of domain specific binding following the thermodynamically-induced rearrangement of the Cu(I) initially from the α domain to the β domain. These previous analytical data extend those reported here and are completely coincident: essentially under all conditions tested, 12 Cu(I) displace 7 Zn (II), minor deviations from a linear relationship can be interpreted in terms of the extent of thermodynamic equilibrium.

Figures 2 and 3 show that even though the Cu(I) atoms are completely bound to the metallothionein within 5 min, emission spectral changes continue to occur for several more hours. In these figures the emission intensity at 600 nm was monitored following the addition of varying amounts of Cu(I) to metallothionein. The 0.0 min point on the x-axis of each plot represents the moment of Cu(I) addition. Note that the y-axes do not always start at zero and are given in arbitrary luminescence intensity units. The actual emission intensity depends on the Cu(I):MT ratio as seen in Figure 1. The vertical bars in Figure 1 show the final Cu(I):MT molar ratios of the data shown in Figures 2 and 3. The kinetic traces (Figures 2 and 3) show the intensity change between the mixing time ($t = 0$ min) and reaction time up to 960 min. The triangles in Figure 1 represent the normalized emission intensities measured between the 5 and

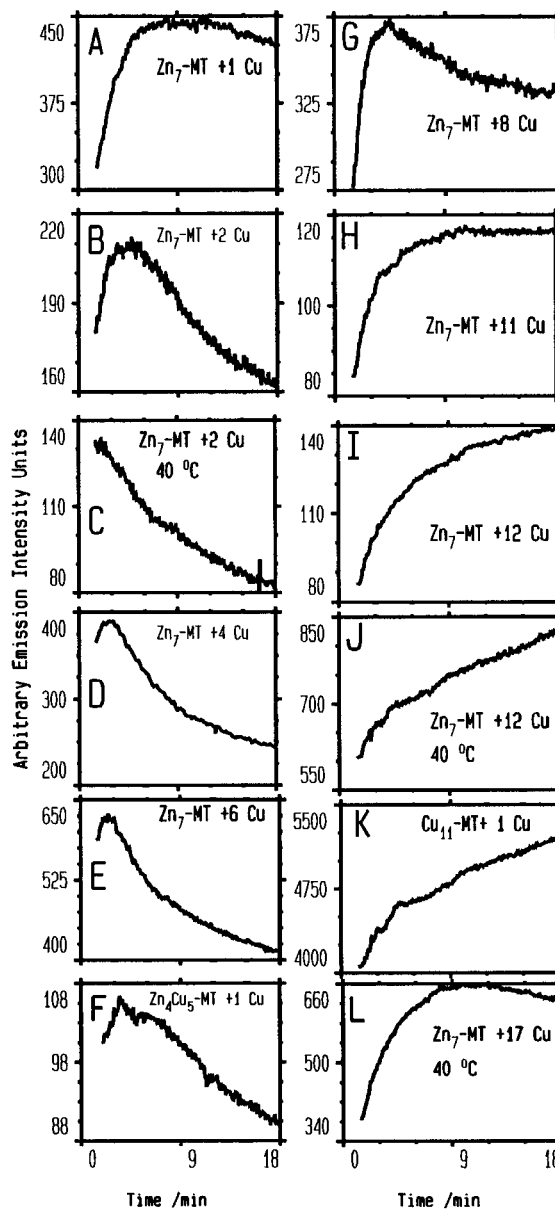


Figure 3. Variation in emission intensity over 18 min following the addition of Cu(I) to MT. The 12 plots (A–L) show the emission intensity measured at 600 nm every 1 s starting 95 s after the addition of Cu(I) to the solution identified on each plot. Note that the y-axes do not start at zero and are plotted in arbitrary emission intensity units. The plots are arranged to show the changes that take place during the 18 min following initial metal binding. In each experiment, a single aliquot containing the stated mol equiv of Cu(I) [(A) 1 at 20 °C, (B) 2 at 20 °C, (C) 2 at 40 °C (D) 4 at 20 °C, (E) 6 at 20 °C, (G) 8 at 20 °C, (H) 11 at 20 °C, (I) 12 at 20 °C, (J) 12 at 40 °C, and (L) 17 at 40 °C] was added to a 10 μ M solution of Zn₇-MT, except for plot F where 1 mol equiv of Cu(I) was added to a 30 μ M Zn₄Cu₅-MT solution at 20 °C, and plot K where 1 mol equiv of Cu(I) was added to a 30 μ M Cu₁₁-MT solution at 20 °C. Note: The minor fluctuations in the signals are due to instrumental instability.

10 minute points in the kinetic plots of Figures 2 and 3. Over time, these intensities change to those represented by the squares in Figure 1 (the intensities at the 30-min points).

The three panels in Figure 2 (A, B, and C) show how the emission intensity of copper-substituted metallothionein varies over long periods of time. Figure 2 shows that the temporal dependence of the emission intensity from Cu(I) bound to the thiolates in metallothionein directly depends on the Cu(I) to MT molar ratio and the temperature. The emission intensity at

600 nm that can only be observed for a shielded Cu–S group either rises rapidly then falls or simply rises over a period of 10 minutes to 16 hours with a characteristic pattern that depends on the Cu(I) to MT molar ratio (rise and fall for Cu:MT < 8, only rises for Cu:MT > 8). These observed changes in the emission intensity mean that the instantaneous environment of the Cu(I) must be changing as a function of time. The time course plotted is 16 h for Figure 2A and 6 hours for Figure 2B,C. The data show how, following an initial rapid increase in intensity that is associated with the Cu(I) binding to the protein (the Cu(I) precursor is nonemissive), the emission intensity changes more gradually to reach an equilibrium value by the end of the monitoring period. It is important to note that the direction of change established after the first 10 min continues until equilibrium is reached. After addition of 1 mol equiv of Cu(I) to an argon-saturated solution of Zn₇-MT in a sealed cuvette (Figure 2A), the emission intensity maximizes after approximately 5 min, then decreases approximately exponentially over 16 h. The low equilibrium intensity is significantly greater than the intensity of Zn₇-MT alone (approximately 0 on the y-axis). After 16 h, the addition of 11 mol equiv of Cu(I) to this Cu₁Zn₆-MT sample results in the emission intensity maximum associated with Cu₁₂-MT. A similar exponential decrease in emission intensity is observed when 2 mol equiv Cu(I) have been added to Zn₇-MT at 2 °C (Figure 2B). In complete contrast, Figure 2C shows that the emission intensity at 600 nm of Zn₇-MT + 11 Cu(I) increases over 4 h.

Figure 3 shows in detail how the temporal variation in emission intensity retains its dependency on the Cu(I):MT molar ratio. The observed emission intensity at 600 nm is plotted as a function of time following the addition of Cu(I) to solutions of metallothionein at 20 and 40 °C. The emission intensity was then measured at 600 nm every 1 s starting 95 s after the addition of the Cu(I). There are four significant trends illustrated by the traces shown in Figure 3.

(1) MT + <8 Cu(I). Those samples containing between 1 and 7 Cu(I) (Figure 3A–F) exhibit a rapid increase in emission intensity in the first 5 min after Cu(I) addition, followed by a steady decrease in intensity. The samples containing >1 Cu(I) (Figures 3B–F) exhibit a much steeper decline in emission intensity than the sample containing only 1 Cu(I) (Figure 3A).

(2) MT + 8 Cu(I). When 8 Cu(I) have been added (Figure 3G), the intensity increases during the first 5 min, after decreasing slightly (~10%), the intensity begins to level off.

(3) MT + 9–12 Cu(I). Following addition of 11 (Figure 3H) or 12 Cu(I) (Figure 3I–K) to a metallothionein solution, the emission intensity increases over the first 5 min and then either levels off (Figure 3H) or continues to increase (by ~40%) (Figure 3I–K) during the next 15 minutes.

(4) MT + >12 Cu(I). When >12 Cu(I) are added to Zn₇-MT (Figure 3L), there is a rapid increase in emission during the first 5 min after the addition. The intensity then remains constant for the remainder of the experiment.

One might expect to observe differences between Cu(I) binding to Zn₇-MT (Figure 3E,I) and Cu(I) binding to Zn_nCu_m-MT (Figure 3F,K). However, we have found that there are *no qualitative differences in the kinetics*. When a single mole equivalent of Cu(I) is added to an equilibrated solution of Zn_nCu_m-MT, the same general trends in the dependence of the emission intensity on time are observed. Figure 3 shows two examples of this type of experiment. In Figure 3F, 1 mol equiv Cu(I) is added to Zn₄Cu₅-MT. As in Figure 3E (Zn₇-MT + 6Cu(I)), after reaching a maximum at 5 min, the emission intensity decreases over the next 15 min. In Figure

3K, 1 mol equiv of Cu(I) is added to a solution of Cu₁₁-MT. As in Figure 3I (Zn₇-MT + 12 Cu(I)), the emission intensity rises rapidly at the beginning and then continues to increase for the entire 18-min period. This provides strong evidence that the temporal changes in emission intensity arise from structural changes associated with binding the newly added Cu(I). That is, the incoming Cu(I) forces changes on the existing Cu–thiolate cluster structure, over and above simply extending the cluster structure.

Parts C, J, and L of Figure 3 show how the emission intensity at 600 nm changes as a function of time at 40 °C when Cu(I) is added in a single aliquot containing (C) 2 mol equiv of Cu(I), (J) 12 mol equiv of Cu(I) or (L) 17 mol equiv of Cu(I) to Zn₇-MT. The initial emission intensity maximum is reached within the 95-s period before data acquisition starts at this temperature. The intensity then *decreases* in a manner similar to that at 20 °C (Figure 3B). When 12 Cu(I) are added to Zn₇-MT at 40 °C (Figure 3J), the emission intensity *increases* for 18 min following the addition of the Cu(I). When 17 Cu(I) are added at 40 °C, the intensity increases sharply and then levels off about 10 min after the addition (Figure 3L).

First-order rate constants (*k*) were derived from the data in Figures 2 and 3. These rate constants are based on the oversimplified assumption that all Cu(I) in the α domain have equivalent luminescent quantum yields and that all Cu(I) in the β domain have equivalent luminescent quantum yields. According to standard kinetic treatments of first order reactions, a plot of $\ln[\text{Int}(t) - \text{Int}(\infty)]$ versus time will have a slope of $-k$ regardless of the initial Cu(I) distribution and the relative luminescent quantum yield of the α and β domains.⁴¹ If not measured, $\text{Int}(\infty)$ can be estimated using the Kezdy–Swinbourne method in which the intensity at time *t* ($\text{Int}(t)$) is plotted versus the intensity at a constant time τ later ($\text{Int}(t + \tau)$). The intersection of the line through the data points with the 45° line gives the value of $\text{Int}(\infty)$.^{41,42} Choosing different values of τ produces variations in the value of $\text{Int}(\infty)$ of approximately 1% which results in a <10% error in the estimation of the rate constants. Figure 4 shows how these methods are applied to the data of Figure 3B (Zn₇-MT + 2Cu(I) at 19 °C) and Figure 3K (Cu₁₁-MT + Cu(I) at 19 °C). Figure 4A illustrates the use of the Kezdy–Swinbourne treatment to yield a value of 124 for $\text{Int}(\infty)$ for the data of Figure 3B. This value is used in the plot of $\ln[\text{Int}(t) - \text{Int}(\infty)]$ shown in Figure 4B. The data can be fit with two linear segments: (i) a short positively-sloped segment through the initial data points, and (ii) a line with a slope of $-1.11 \times 10^{-3} \text{ s}^{-1}$ fit through the decreasing data. The slope of the line through the data at longer times directly yields the rate constant of the slower step of the reaction (k_s). The contribution of the slower step to the early part of the data must be subtracted from the observed data before obtaining the rate constant of the faster step (k_f).⁴¹ The contribution of the fast component of the data can be defined by Δ , where Δ is the difference between the initial observed data points and the extrapolation of the long-time line to earlier times.⁴¹ The resulting plot of $\ln \Delta$ versus time for the data between 1.5 and 3 min (shown as the inset in Figure 4B) yields a value of k_f of $1.28 \times 10^{-2} \text{ s}^{-1}$. This treatment can be applied to all the kinetic data of this paper including that shown in Figure 3H–K in which the intensity continues to increase for the entire 20 min. In these latter cases, $\ln[\text{Int}(\infty) - \text{Int}(t)]$ is plotted versus time in order to obtain the rate constants k_f and k_s , as shown in Figure

(41) Espenson, J. H. *Chemical Kinetics and Reaction Mechanism*; McGraw-Hill Book Company: Toronto, Canada, 1981.

(42) Swinbourne, E. S. *J. Chem. Soc.* **1960**, 2371–2372.

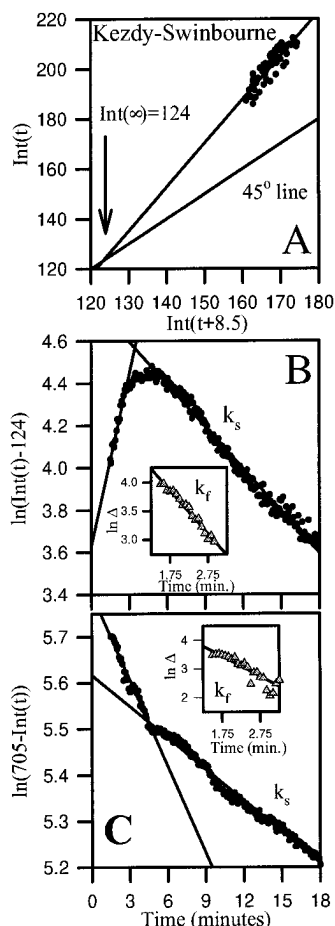


Figure 4. Example of kinetic treatment of data. (A) Kezdy–Swinbourne treatment of the data shown in Figure 3B, Zn₇-MT + 2Cu(I) at 20 °C. The plot shows the intensity at time t ($\text{Int}(t)$) vs the intensity 8.5 min later ($\text{Int}(t + 8.5)$) (shown by the circles) intersecting with the 45° line at 124 intensity units ($\text{Int}(\infty)$). (B) Plot of $\ln[\text{Int}(t) - \text{Int}(\infty)]$ versus time for the data shown as Figure 3B. (C) Plot of $\ln[705 - \text{Int}(t)]$ (where $\text{Int}(\infty) = 705$) vs time for the data shown in Figure 3K (Cu₁₁-MT + Cu(I) at 20 °C (note: the intensities in Figure 3K were multiplied by 0.1 for this analysis). In both B and C, the fits through the two data sets indicate the biphasic nature of the change in emission intensity. The slope of the line through the latter data (from 5.5 to 18 min) gives the rate constant of the slowest step (k_s). The insets show the plots of $\ln \Delta$ vs time and the corresponding rate constant (k_f) where Δ is the difference between the observed data points between 1.5 and 3 min and the extrapolation of the long-time line. In all plots, only every fifth datum point is displayed for clarity of presentation.

4C. The results from similar kinetic treatments of all raw data in are given in Table 2.

Discussion

Although the stability constants of metals bound in the metal–thiolate clusters of metallothionein are high (10^{15} for Cd²⁺), spectroscopic evidence suggests that these metals are quite labile. CD and ¹¹³Cd NMR spectroscopic studies indicate that at room temperature Cd(II) displaces Zn(II) from Zn₇-MT in a random manner, with Cd(II) atoms binding evenly distributed across the two domains of the protein.^{3,8,17} If the temperature is raised, the metallothionein-bound Cd(II) and Zn(II) rearrange from this distributed species into the domain-specific species with a filled Cd₄- α domain, as found naturally.^{3,17} The presence of a carrier such as EDTA during the digestion of the Cd-substituted protein with subtilisin catalyzes the rearrangement of the metals from the kinetic product to the thermody-

Table 2. Observed Rate Constants (k_f and k_s) for the Binding and Rearrangement of Cu(I) to Metallothionein^a

solution	conditions ^b	raw data	$10^2 k_f$ (s ⁻¹)	$10^3 k_s$ (s ⁻¹)
Zn ₇ -MT + Cu(I)	30 μ M	Figure 2A	0.67	0.19
Zn ₇ -MT + 2Cu(I)	2 °C	Figure 2B	0.12	0.11
	19 °C	Figure 3B	1.28	1.11
	40 °C	Figure 3C	<i>c</i>	1.63
Zn ₇ -MT + 4Cu(I)		Figure 3D	2.28	2.65
Zn ₇ -MT + 6Cu(I)		Figure 3E	3.85	2.45
Zn ₄ ,Cu ₅ -MT + Cu(I)	30 μ M	Figure 3F	1.03	1.42
Zn ₇ -MT + 8Cu(I)		Figure 3G	2.19	1.68
Zn ₇ -MT + 11Cu(I)		Figure 3H	0.74	<i>d</i>
Cu ₁₀ ,Zn ₁ -MT + Cu(I)	6 °C	Figure 2C	0.30	0.14
Zn ₇ -MT + 12Cu(I)	19 °C	Figure 3I	0.39	2.38
	40 °C	Figure 3J	<i>c</i>	2.51
Cu ₁₁ -MT + Cu(I)	30 μ M	Figure 3K	1.15	0.38
Zn ₇ -MT + 14Cu(I)		not shown	3.00	<i>d</i>

^a Kinetic parameters derived from the data of Figures 2 and 3. ^b Data were obtained at 19 °C with a metallothionein concentration of 10 μ M unless otherwise noted. ^c k_f was not determined at 40 °C since this step occurred before the start of data collection. ^d k_s could not be determined for these reactions due to one of two possibilities: (i) the reaction is actually monophasic or (ii) the second step occurs very quickly and could not be observed.

namically stable, domain-specific species.⁴³ Although the stable thermodynamic product following metal rearrangement can be detected by allowing the protein to reach equilibration, the direct observation of the migration of metals within metallothionein shortly after binding has not previously been reported. In the experiments described here, the emission intensity of the copper-substituted metallothionein is used to monitor the copper–thiolate structures formed following mixing.

Rearrangement of Cu(I) in MT at High Temperatures.

We have previously reported that the binding of Cu(I) to Zn₇-MT in aqueous solution involves a rearrangement from a kinetically-controlled distributed product to a thermodynamically-controlled domain-specific product.¹⁹ This was determined in part by making sequential additions of Cu(I) to Zn₇-MT at 10 and 40 °C and measuring the emission spectrum after each addition. The effect of the degree of Cu(I) loading on the normalized emission intensity at λ_{max} is summarized in Figure 5. These data are displayed so that the emission intensities at the 1 Cu(I) point are equivalent in order to remove the effect of increased thermal solvent deactivation at higher temperatures (which decreases the absolute intensity at all Cu(I):MT molar ratios). The observation of the maximum in emission intensity at the 12 Cu(I) point in the titration corresponds with the formation of a Cu₁₂-MT species with two copper–thiolate clusters that are protected from solvent access by the protein backbone.^{19,20} As more Cu(I) is added (from 12 to 18 mol equiv), the decreasing emission intensity indicates that the tight cluster structure opens to allow greater solvent access.¹⁹

The difference in the pattern of normalized intensities for the titrations carried out at 10 and 40 °C indicate that the Cu₁₂-MT structure must form differently at the two temperatures. At 10 °C, the quantum yield per Cu(I) increases reasonably linearly as 1–7 mol equiv of Cu(I) are added to Zn₇-MT, whereas, at 40 °C, the quantum yield per Cu(I) actually decreases as 2–7 mol equiv of Cu(I) are added (Figure 5). At high temperatures, equilibration to the thermodynamically-controlled product occurs rapidly. The formation of the Cu₆- β domain from the reconstitution of the whole protein with 6 Cu(I) detected under the relatively harsh conditions of proteolysis indicates that this thermodynamically-controlled product of Cu(I) binding to

(43) Stillman, M. J.; Zelazowski, A. J. *Biochem. J.* **1989**, *262*, 181–188.

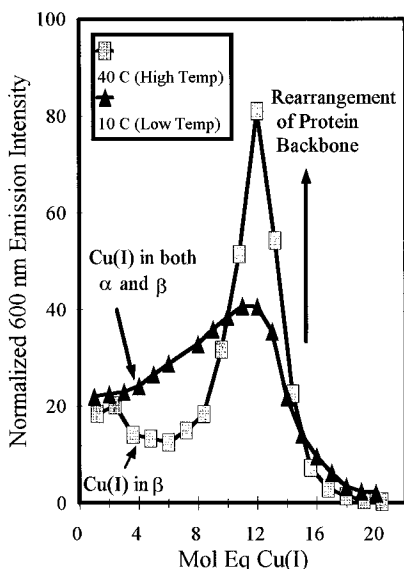


Figure 5. Normalized emission intensities as a function of mol equiv of Cu(I) at 40 °C and at 10 °C. This is a summary of data reported in ref 19. Cu(I) was added in sequential approximate mol equiv aliquots to a solution of Zn₇-MT at the stated temperature. After each addition, the emission spectrum was obtained after a 5 min equilibration time. The normalized intensity represents the emission intensity at λ_{max} divided by the mol equiv of Cu(I). The data is displayed so that the intensities for 1 mol equiv of Cu(I) are equivalent to account for the differences in thermal solvent deactivation at the two temperatures.

metallothionein involves Cu(I) binding exclusively to the β domain for 1–6 Cu(I).^{21,44} At low temperatures, equilibration to the thermodynamic product occurs much more slowly and the kinetically-controlled product dominates. We have previously reported that this product involves Cu(I) filling both the α and β domains statistically in the so-called distributed manner.^{19,20} The decrease in the normalized emission intensities at 40 °C between 1 and 6 mol equiv of Cu(I) added must then be caused by Cu(I) binding in the β domain indicating that, in the whole protein, Cu(I)–thiolate clusters in the α domain emit more strongly than those in the β domain by a factor of about 10.¹⁹ The temperature dependence data shows that Cu(I) initially binds across both domains at all temperatures, followed by a rapid redistribution of Cu(I) to the β domain at high temperatures.¹⁹

Qualitative Interpretation of Luminescence Time Dependence. The data from this study (Figure 1) indicate that the rearrangement of the bound Cu(I) also occurs at room temperature, but at a much slower rate (30 vs 5 min). In the experiments portrayed in Figures 2 and 3, we monitor the change in emission intensity at 600 nm with time after the addition of Cu(I) to metallothionein.

Following the addition of Cu(I) to Zn₇-MT, we might expect the emission intensity to change with time according to one of the selected scenarios shown in Figure 6. If the Cu(I) initially binds to the protein in the most thermodynamically stable manner, we would expect to see a plot similar to that seen in Figure 6A. In this model, the emission intensity increases as the Cu(I) binds to the Zn₇-MT and then remains constant when all the Cu(I) is bound. Parts B and C of Figure 6 show plots expected for a rearrangement from a highly emissive copper–thiolate cluster to a less emissive cluster environment. Again the emission intensity increases over the first 5 min as the Cu(I) binds to the protein. After the Cu(I) is bound in a

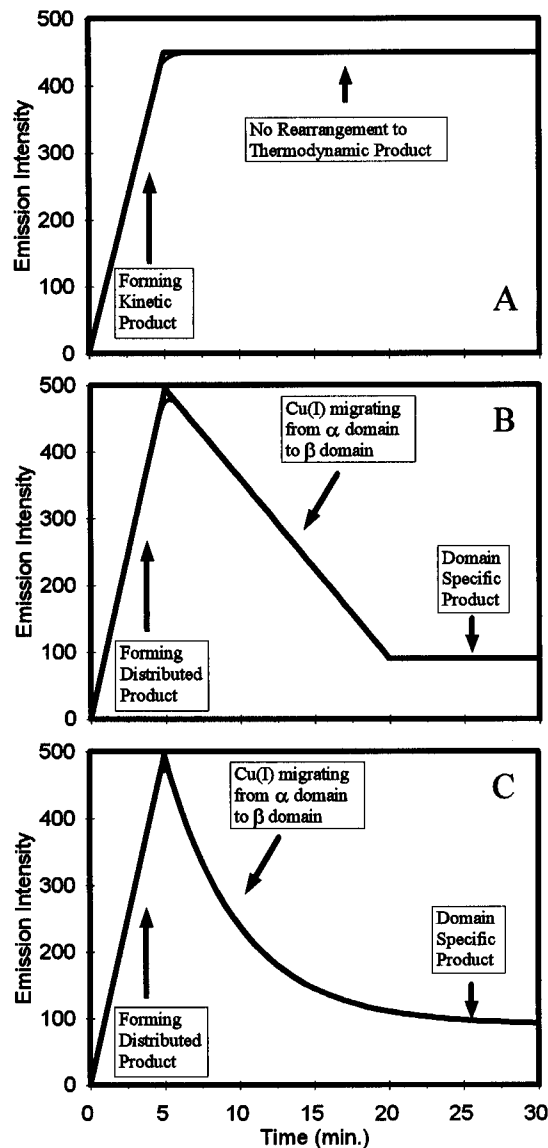


Figure 6. Predicted change in emission intensity as a function of time following addition of Cu(I) to metallothionein. Calculated variations in the emission intensity recorded at 600 nm from Cu-MT at room temperature following addition of 6Cu(I) to Zn₇-MT are shown. The first step in each case is the formation of the kinetic product which is accompanied by an overall increase in emission intensity during the first 5 minutes of the reaction. (A) No further rearrangement occurs. For calculations shown in parts B and C, the temporal effects on the emission intensity of subsequent rearrangements by zero order (B) or first order (C) kinetics is shown. The region after 5 min in each plot was calculated using initial Cu(I) concentrations of 30 μM in each domain and assigning each mol equiv of Cu(I) (i.e. 10 μM) in the α domain an emission intensity of 150 and each Cu(I) in the β domain an emission intensity of 15. The total emission intensities after 5 min were determined based on calculations of the concentration of Cu(I) in each domain following (B) a zero-order rate equation with $k = 2 \mu\text{M}/\text{min}$ and (C) a first-order rate equation with $k = 0.2 \text{ min}^{-1}$.

distributed manner (the kinetically-controlled product), the Cu(I) migrates to fill the less emissive β domain (the domain specific product). Theoretical decreases in the emission intensity are shown for a redistribution of 6 Cu(I) following zero-order (Figure 6B) or first-order (Figure 6C) kinetics. The curves beyond 5 min were calculated as follows. (i) At a time of 5 min, the concentration of Cu(I) in the α and β domains was assumed to be equal (30 μM –3 mol equiv in each domain of a 10 μM solution of protein). (ii) The emission intensity was approximated by arbitrarily assigning each mol eq Cu(I) (i.e. 10 μM) in the α domain an average intensity of 150 and each

(44) Kille, P.; Lees, W. E.; Darke, B. M.; Winge, D. R.; Dameron, C. T.; Stephens, P. E.; Kay, J. J. *Biol. Chem.* **1992**, 267, 8042–8049.

Cu(I) in the β domain an average intensity of 15. (Of course, from the data we can see that this last approximation is invalid since if all Cu(I) in the β domain contributed equally to the emission, the 40 °C curve in Figure 5 would be a horizontal line from 1 to 6 Cu(I); however, the use of this assumption simplifies the model.) (iii) In the case of zero-order kinetics (Figure 6B), the concentration of Cu(I) in each domain after 5 min was calculated using an arbitrary rate of 2 $\mu\text{M}/\text{min}$ as the rate of decrease of Cu(I) in the α domain (which must equal the rate of increase of Cu(I) in the β domain). After 20 min, all 6 Cu(I) would be in the β domain and the emission would remain constant. (iv) In the case of first-order kinetics (Figure 6C), the concentration of Cu(I) in the α domain is equal to $[30 \mu\text{M}]e^{-kt}$ where k was given an arbitrary value of 0.2 min^{-1} and t is the actual time (-5 min). The concentration of Cu(I) in the β domain is then $60 \mu\text{M}$ minus the concentration of Cu(I) in the α domain.

The actual data in Figures 2 and 3 display examples of the scenarios portrayed in Figure 6A,C, plus an additional scenario. At room temperature (20 °C), all of the reactions appear to be biphasic (Figure 3). The initial step is associated with a steep and steady increase in the emission intensity and occurs in the first five minutes following the addition of Cu(I). After that, the direction of the change in emission intensity depends upon the degree of copper loading. Emission from samples with <8 Cu(I) (Figure 3A,B,D–F) *slowly decreases* in intensity over 18 min (similar to the scenario shown in Figure 6C). The emission from solutions with between 9 and 12 Cu(I) (Figure 3H,I,K) *increases slowly* (when compared to the rapid increase of the first 5 min) over 18 min (the new scenario). The data for $\text{Zn}_7\text{-MT} + 8\text{Cu(I)}$ (Figure 3G) may indicate a “crossover” point when 8 Cu(I) are present. The emission intensity levels off after only 10 min instead of continuing to decrease for the entire 18 min. This “dividing line” between spectroscopic properties has been seen previously in differing temperature cycling effects on the luminescence spectra of copper-containing metallothioneins¹⁹ and in the formation of a highly chiral $\text{Cu}_9\text{Zn}_2\text{-MT}$ species at high temperature²⁰. When >12 Cu(I) are bound to the metallothionein (Figure 3L), the emission intensity varies *only slightly* ($\pm 5\%$) within 18 min after the addition of Cu(I) (similar to the scenario shown in Figure 6A), *decreasing* only when further copper is added. The stability of these latter species indicates that neither the Cu(I) nor the protein has been oxidized since oxidation would result in a rapid decrease in emission signal as the oxidized protein released Cu(I).

Physical Interpretation of k_f . The changes observed in the emission intensity with time following the addition of Cu(I) to $\text{Zn}_7\text{-MT}$ and the observed rate constants can be interpreted in terms of changes in the configuration of the protein from a kinetically-controlled product to a thermodynamically more stable product. The initial step, proceeding with a rate constant k_f , can be associated with the initial binding of Cu(I) to $\text{Zn}_7\text{-MT}$ in a domain-distributed manner. At room temperature, the formation of this domain-distributed kinetic product is essentially complete in 5 min as indicated by the initial steep rise in emission intensity due to unique Cu–S groups in solvent-isolated sites. The metal analysis data in Table 1 show that for $\text{Zn}_7\text{-MT} + 12 \text{ Cu(I)}$, all the Cu(I) ions are indeed bound to the protein within 5 min. Since k_f for $\text{Zn}_7\text{-MT} + 12 \text{ Cu(I)}$ has a lower value than that for any of the other solutions (see Table 2), the Cu(I) should be bound within 5 min in all the other solutions also. The rate of formation of this kinetic product should increase with temperature. The data summarized in Table 2 show that this indeed is the case. At 2 °C, the initial

binding reaction of 2 mol equiv of Cu(I) to $\text{Zn}_7\text{-MT}$ (Figure 2B) is slowed by a factor of 10 compared to the reaction at room temperature. At 40 °C (Figure 3C), the reaction occurs too quickly for us to observe the initial formation of the kinetic product. As seen in Figure 3C, the initial rise in emission intensity has already occurred by the time our data acquisition begins, 95 s following the addition of 2 mol equiv of Cu(I) to $\text{Zn}_7\text{-MT}$. Kinetic analysis confirms the monophasic nature of the data at 40 °C (Table 2). The single rate constant obtained at 40 °C can be associated with the slower room temperature step (k_s).

Although direct comparison of the values obtained for the rate constants are difficult due to the assumption of equal luminescent quantum yields of every $\beta\text{-Cu}$ and every $\alpha\text{-Cu}$, examination of Table 2 yields some interesting trends in k_f . It appears that the rate of domain-distributed Cu(I) binding depends not only on the concentration of Cu(I) added, but also on the structure of the species being formed. When 1–6 mol equiv of Cu(I) are added to 10 μM $\text{Zn}_7\text{-MT}$, the rate constant of binding on a per Cu basis is $(6.3 \pm 0.4) \times 10^{-3} \text{ s}^{-1}$. Similarly, when a single 30 μM aliquot of Cu(I) is added to either 30 μM $\text{Zn}_4\text{Cu}_5\text{-MT}$ or $\text{Cu}_{11}\text{-MT}$, k_f is approximately 10^{-2} s^{-1} . When 8–12 mol equiv of Cu(I) are added, this per Cu rate constant decreases appreciably. A possible explanation is the difference in cysteine binding modes with a low or high number of Cu(I) mole equivalents present. When each domain is only half full or less than half full, no $\text{Cu-S}_{\text{cys}}\text{-Cu}$ bonds have formed yet. Each Cu(I) is bound to either a terminal S_{cys} or to one which is bridging to Zn(II) ($\text{Cu-S}_{\text{cys}}\text{-Zn}$). Thus, each Cu(I) coming into the protein will bind in this simple manner at about the same rate. When each domain is more than half full, $\text{Cu-S}_{\text{cys}}\text{-Cu}$ bridges must form and the rearrangement needed to accommodate the incoming Cu(I) is more complex causing k_f to decrease.

Physical Interpretation of k_s for the Addition of <8 mol equiv of Cu(I) to MT. While k_f can provide significant details concerning the initial binding of Cu(I), similar details can be derived from k_s only following determination of the physical origin of this slower step. Since the metal displacement studies (Table 1) indicate that all the Zn(II) ions have been displaced, this second rate constant is not simply the result of biphasic metal displacement, such as that observed with $\text{Zn}_n\text{Cd}_m\text{-MT}$ and gold sodium thiomalate.⁴⁵ The changes in the emission intensity over the 18 min period following the binding of 1–8 mol equiv of Cu(I) to $\text{Zn}_7\text{-MT}$ can be interpreted as follows. After formation of the kinetic product, further changes in the emission intensity indicate that the Cu(I) atoms and the peptide rearrange to form a more stable product. From parts B and C of Figure 3, it is clear that, after the first two Cu(I)s bind randomly across the two domains in $\text{Zn}_7\text{-MT}$, Cu(I) atoms move to a more exposed site (as indicated by a decrease in emission intensity) in the thermodynamic product. The decrease in emission with time as 2–7 mol equiv of Cu(I) are added to $\text{Zn}_7\text{-MT}$ must arise from the migration of Cu(I) from the α domain in the kinetically-controlled domain-distributed product to fill the less emissive β domain in the domain-specific thermodynamically-controlled product. k_s is thus the rate constant for the migration of Cu(I) from the α domain to the β domain. The formation of the domain-specific thermodynamic product should dominate at higher temperatures while the domain-distributed kinetic product should dominate at lower temperatures. Indeed, the $\text{Cd}_4\text{-}\alpha$ cluster, the thermodynamic product of Cd(II) binding to $\text{Zn}_7\text{-MT}$, does not form below 5

(45) Shaw, C. F., III; Laib, J. E.; Savas, M. M.; Petering, D. H. *Inorg. Chem.* **1990**, *29*, 403–408.

°C because at least one Zn(II) remains bound to the α domain sufficiently tightly to resist replacement below 5 °C.¹⁷ A similar preference for the domain-specific product at higher temperatures has also been reported for the binding of Cu(I) to Zn₇-MT¹⁹ and is also evident in this study from the data in Table 2. When 2 mol equiv of Cu(I) have been added to Zn₇-MT, k_s , the rate of Cu(I) redistribution from the α domain to the β domain, increases dramatically upon increasing the temperature from 2 to 19 to 40 °C. A plot of $\ln(k_s/T)$ vs $1/T$ yields the activation enthalpy and entropy, ΔH^\ddagger and ΔS^\ddagger for this process. a ΔH^\ddagger value of 50 kJ/mol was obtained from the slope of this plot and a ΔS^\ddagger value of $-140 \text{ J K}^{-1} \text{ mol}^{-1}$ from the intercept. These values are comparable to those values obtained for the reaction between DTNB and MT.⁴⁶ The negative value for ΔS indicates the entropically unfavored nature of the rearrangement.

Physical Interpretation of k_s for the Addition of >8 Cu(I) to MT. The effect of Cu(I) moving from the α domain to the β domain cannot alone explain the phenomena seen when between 9 and 12 mol equiv of Cu(I) are added to metallothionein (Figure 3H–K). It is also significant that the emission intensity increases even when 12 Cu(I) have been added (Figure 3I–K). At this level of copper loading, the kinetically-controlled product can be superficially formulated as the same as the thermodynamically-controlled product— $(\text{Cu}_6)^\alpha(\text{Cu}_6)^\beta$ -MT; however, the increase in intensity with time indicates that the structures are not exactly the same. The explanation must lie in the differing coordination geometry of Cu(I) and Zn(II). The presence of trigonal (for the Cu), compared with tetrahedral (for the Zn) geometry, requires major changes in the arrangement of the cysteinyl thiolates of Zn₇-MT. A similar rearrangement has been observed as Hg(II) is added to Zn₇-MT. The peptide chain rearranges around different metal–thiolate cluster structures as the coordination geometry of the Hg(II) changes from distorted tetrahedral to trigonal to digonal as Hg(II) is added to

Zn₇-MT to form Hg₇-MT, Hg₁₁-MT, and Hg₁₈-MT, respectively.^{47,48} Through the temporal changes in emission intensity (Figure 3H–K), we can observe the conformational rearrangement of the protein backbone in Cu-MT. As the binding site structure is tightened and solvent access restricted, the emission intensifies. This conformational rearrangement of the protein backbone occurs slightly more rapidly at high temperatures (30% increase at 40 °C in Figure 3J) than at low temperatures (20% increase at 20 °C in Figure 3I) resulting in a 5% increase in k_s for Zn₇-MT + 12Cu(I). This more rapid rearrangement of the peptide chain at higher temperatures results in the extreme increase in the quantum yield of emission as 8 to 12 Cu(I) are added to Zn₇-MT at 40 °C as compared to that obtained at 10 °C (Figure 5).¹⁹ These data then are evidence that the copper–thiolate cluster structures are dynamic in the binding site; different structures are adopted, driven by the lower free energy of the new product. At elevated temperatures sufficient thermal energy is available to exceed activation energy barriers to the rearrangement of the peptide chain that is required if cysteinyl thiolates move within three-dimensional space.

Acknowledgment. We acknowledge useful discussions with Dr. Anthony Presta at U.W.O. and the assistance of John Dixon at U.W.O. with data presentation. We thank the Natural Sciences and Engineering Research Council of Canada for financial support of this work in the form of an operating grant (to M.J.S.) and a Graduate Scholarship (to ARG). We also thank the Center for Chemical Physics at U.W.O. for continued support of our work. M.J.S. is a member of the Center for Chemical Physics and the Photochemistry Unit at U.W.O. This is publication No. 499 of the Photochemistry Unit.

IC950540A

(46) Zhu, Z.; Goodrich, M.; Isab, A. A.; Shaw, C. F., III. *Inorg. Chem.* **1992**, *31*, 1662–1667.

(47) Lu, W.; Stillman, J. J. *J. Am. Chem. Soc.* **1993**, *115*, 3291–3299.

(48) Lu, W.; Zelazowski, A. J.; Stillman, M. J. *Inorg. Chem.* **1993**, *32*, 919–926.